



The Effect of Wall's Porous Liner on MHD Couette Flow of Carreau Fluid in an Inclined Channel under the Convective Conditions

Tamara Shihab Alshareef 

Department of Mathematics, Collage of Education for Pure Science Ibn Al-Haitham, University of Baghdad, Baghdad 009641, Iraq

Corresponding Author Email: tamara.s.a@ihcoedu.uobaghdad.edu.iq

Copyright: ©2024 The author. This article is published by IIETA and is licensed under the CC BY 4.0 license (<http://creativecommons.org/licenses/by/4.0/>).

<https://doi.org/10.18280/ijht.420107>

ABSTRACT

Received: 4 September 2023

Revised: 11 November 2023

Accepted: 15 January 2024

Available online: 29 February 2024

Keywords:

Carreau fluid, Couette flow, Pours liner, heat transfer, slip boundary conditions

Present work discusses the effects of channel wall thickness on MHD flow employing permeability effect on porous wall liner. Couette steady Carreau fluid flow in a parallel inclined plate's channel at an inclination λ to the horizontal. We also examined how tilted magnetic fields affect channel flow with slope angle β . We employ slip boundary conditions. Convective boundary conditions affect heat transmission. An incompressible Carreau fluid's governing system equations are in Cartesian coordinates. Low Reynolds number and negligible inertial effects progress the problem formulation. Similarity of non-dimensional quantities converts flow controlling equations into conventional differentiation equations. Series solutions for axial velocity are obtained analytically by regular perturbation technique method (RPTM) when Weissenberg number is small, while the energy equation is solved numerically by "Explicit Euler" method with size step of (0.1). Plotting graphs shows the effects of Hartmann number, Darcy number, channel and magnetic field inclination angles, and others on velocity and temperature distributions by using Mathematica program software.

1. INTRODUCTION

Due to its usefulness in numerous fields of industry and technology, non-Newtonian fluids have recently attracted a lot of attention from the scientific community. Blood, honey, shampoo, ketchup, paints, mud, and polymer melts are all examples of non-Newtonian fluids since their viscosity varies with the applied force. Because of their complexity, non-Newtonian fluids can be categorized into two types: those whose shear stress depends solely on the shear rate and those with both elastic and viscous properties. Therefore, the expected behavior of this fluid type is described by many fluids. Many researchers have dealt with various types of non-Newtonian fluids for different flows and using analytical and numerical methods [1-4]. One such model is the Carreau fluid, a generalized Newtonian fluid whose viscosity varies with the shear rate; this model is particularly well-suited to representing fluid movement in the high-shear-rate regime. Carreau pioneered the use of molecular network theory in rheological equations [5]. Because of these uses, Carreau fluid flow has been the subject of much research in a large number of different geometries. It is common knowledge that fluid dynamics when surrounded by a magnetic field, play an important role in numerous scientific and technological procedures. (MHD) pumps, accelerators, power generators, aerodynamic heating, and polymer technologies are all examples of these uses. Pump meters, cell separators, heat exchangers, magnetic drugs, and magnetic tracers used for precise homing all make use of the principles of magnetic field

engineering (MHD) [6]. A multitude of researchers have looked at MHD. in various fluid flows in light of these potential uses. Akbar et al. [7] a conduit allows for the passage of an electrically conducting viscoelastic fluid as well as the transmission of heat. has been theoretically investigated (MHD). Hayat et al. [8] provide research on the impact of a generated magnetic field on the peristaltic movement of Carreau fluid. Prakash et al. [9] investigated the waveform transport of Carreau fluid in an asymmetric tapered channel using the effects of a uniform magnetic field. The peristaltic movement of a Carreau fluid through a non-uniform conduit is shown to be affected by an angled magnetic field by Ahmed [10], for more references on this side [11-15]. Fluid cooling and heating are common tasks in many manufacturing and chemical processes. Extrusion is a common procedure used in the plastics and food processing industries. The rate of heat transport and the distribution of temperatures must be understood with thermally sensitive goods like food and pharmaceutical products, and the maximum allowable temperature must not be raised. In the polymer business, knowing the rate of heat transmission and temperature distribution profile is crucial since it has a major impact on the uniformity of the finished products [16, 17]. The appropriate pumping of groundwater can help alleviate water scarcity issues, and this is where the research of input through a porous media comes in. Biologists have found the flow of water through porous plant material to be fascinating. Channebasappa et al. [18] studied how the measurement of the porous material's thickness affected the flow in a canal with

parallel plates. When a porous coating that is impervious to erosion is installed in the channel walls. Similar to what Kumaraswamy Naidu and others have done [19] was looked at. Jeffrey fluid speed in a parallel plate channel lined with an absorbent material that doesn't erode depends on the depth of the pore structure [20-22]. Couette flow, one of the fundamental flows, has piqued the interest of fluid dynamics experts. As a result of its potential utility in a variety of technological and industrial contexts. What we have here is the movement of two surfaces separated by a viscous fluid, with one of those surfaces moving tangentially with respect to the other. Shear stress is applied to the fluid and produces flow as a result of the motion of the surfaces. Additionally, there may be a pressure gradient that is applied in the direction of flow, albeit this depends on the precise meaning of the term Injection molding [23]. The manufacturing processes under consideration include flow molding, blow molding, and continuous casting., forming plastic, extraction, asthenosphere, and extrusion flows are all examples of one-directional flows utilized in a variety of industries [24]. The governing differential equations for such a flow may also yield accurate solutions, which can be used to complement the outcomes of the flow issue when dealing with complex geometries. You can see further reading in this area [25, 26]. For more references in this field can see the studies of Nadeem et al. [27], Rickert et al. [28], and Niranjana et al. [29]. This work presents the results of a theoretical investigation into the impact or influence of an inclined magnetic field on the Couette steady flow of conducting Carreau fluid in a sloping channel made up of parallel plates. Flow modification due to slip boundary circumstances. The use of convective boundary conditions for heat transport aids in this investigation. By using approximation and numerical techniques, the governing equations of motion and energy can be solved. What follows are the remaining sections of this paper: The mathematical formulation of the problem is presented in section (2). In section (3), we examine the system of motion and energy equations that control the situation. Shear stress constitutive equations for Carreau fluid are presented in section (4). The solutions to the problems are shown in section (5). Sections (6) and (7) analyze the numerical findings of the parameters and the conclusions.

2. MODELLING THE ISSUE MATHEMATICALLY

Let us examine the Couette inflow of conductivity that doesn't compress Carreau fluid and fills the inclined channel content of parallel plates. In contrast, the one above maintains a steady speed u_0 while the lower one is at rest, and the end part of it is lined with porous material. The channel of the flow is sloped with the horizontal by an angle denoted by α . Let h^* be the dimension of the flow's breadth area that is unrestricted higher than the porous surface and δ^* proportional to the size of the porous liner in width. Between parallel plates, a constant flow in one direction, the velocity field $\vec{V} = (u(y), 0, 0)$ satisfied the continuity equation. In order to calculate this field of velocity, we will assume that the fluid has some level of electrical conductivity and that an external transverse uniform continuous magnetic field of intensity is expanding the channel as it moves in this direction, B_0 . In addition, because of the low magnetic Reynolds number, the induced magnetic field is not taken into consideration. As a result, the total magnetic field, which is influenced by the flow in a sloping

way and is inclined with an inclination angle given by (β) , is what is taken into consideration. So, the overall of the magnetic field vector becomes $B=(0, \beta_0, 0)$. It is also presumed that there is no electrical field that is,

$$\vec{J} = \sigma(\vec{E} + \vec{V} \times \vec{B}), \quad (1)$$

\vec{J} the current vector σ is the fluid's electrical conductivity and \vec{E} is the electrical field. So, Eq. (1) gives:

$$\vec{J} \times \vec{B} = (-\sigma B_0^2 \cos^2(\beta) \bar{u}, 0, 0) \quad (2)$$

In this work, let T_0 the temperature be measured in the layer below the porous one, which T_1 is the temperature of the moving uppermost layer. The direction of the flow is given by the X-axis, which is the distance (2h) between the lower thin plate and the upper plate of one of the channels (see Figure 1).

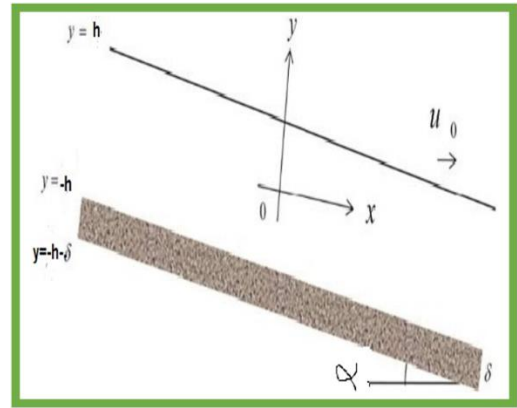


Figure 1. Physical model

3. SYSTEM OF THE PROBLEM'S CONTROLLING EQUATIONS

The governing equations for the flow in the fixed frame are:
Continuity equation:

$$\frac{\partial \bar{u}}{\partial x} = 0 \quad (3)$$

$$0 = -\frac{\partial \bar{P}}{\partial X} + \frac{\partial}{\partial Y} \tau_{XY} - \sigma B_0^2 \cos^2(\beta) \bar{u} + \rho g \sin \alpha \quad (4)$$

$$\rho c_p \left(\frac{\partial \bar{T}}{\partial t} + \bar{u} \frac{\partial \bar{T}}{\partial X} \right) = K_1 \left(\frac{\partial^2 \bar{T}}{\partial Y^2} \right) + \tau_{XY} \frac{\partial \bar{u}}{\partial Y} +$$

$$\sigma B_0^2 \cos^2(\beta) (\bar{u})^2 - \frac{\partial}{\partial Y} q_r \quad (5)$$

in which, $\frac{\partial}{\partial Y} q_r = 4\lambda^2(T_0 - T)$.

Considering the following problem-specific border conditions:

$$\begin{aligned} \bar{u} &= u_0 & \text{at } \bar{Y} &= h \\ \frac{\partial \bar{u}}{\partial Y} &= \frac{\alpha_1}{\sqrt{k_0}} \bar{u} & \text{at } \bar{Y} &= -h \end{aligned} \quad (6)$$

$$\begin{aligned}
-k_r \frac{\partial T}{\partial Y} &= h_r (T_0 - T) & \text{at } \bar{Y} = -h & & \frac{\partial u}{\partial x} &= 0 \\
k_r \frac{\partial T}{\partial Y} &= h_r (T - T_1) & \text{at } \bar{Y} = h & & &
\end{aligned} \tag{7}$$

$$\begin{aligned}
u &= \frac{\bar{u}}{u_0}, x = \frac{\bar{X}}{h}, y = \frac{\bar{Y}}{h}, p = \frac{h\bar{P}}{\mu_0 u_0}, \\
\text{We} &= \frac{\Gamma u_0}{h}, \text{Dr} = \frac{h}{\sqrt{k_0}} = \frac{1}{\text{Da}}, t = \frac{\bar{t} u_0}{h}, \\
\text{Re} &= \frac{\rho h u_0}{\mu_0}, M = \sqrt{\frac{\sigma}{\mu_0}} B_0 h, \theta = \frac{T - T_0}{T_1 - T_0}, \\
\text{Fr} &= \frac{u_0^2}{gh}, \rho_r = \frac{\mu_0 c \rho}{k_1}, \tau_{\bar{X}\bar{Y}} = \bar{\tau}_{\bar{X}\bar{Y}} \\
&= \frac{\mu_0 \mu_0}{h} \tau_{XY}, \dot{y} = \frac{h}{u_0} \dot{y} \text{Ec} = \frac{u_0^2}{c \rho (T_1 - T_0)}, \\
\Gamma &= \frac{\text{Re}}{\text{Fr}}, \text{Bh} = \frac{h \mu_0}{kr}, \text{Br} = \rho r \text{Ec} = \frac{\mu_0 \mu_0^2}{k_1 (T_1 - T_0)}, \\
\text{Nr} &= \frac{2\lambda h}{\sqrt{k_1}}
\end{aligned} \tag{8}$$

In the following table, we are given the physical nomenclature of the used parameters.

4. CONSTITUTIVE EQUATION FOR THE SHEAR STRESS OF CARREAU FLUID

The Carreau fluid can be represented by the following form of the constitutive equations [9]:

$$\bar{\tau} = (\mu_\infty + (\mu_0 - \mu_\infty) (1 + (\bar{\Gamma} \dot{y})^2)^{\frac{n-1}{2}}) \dot{y} \tag{9}$$

where, $\bar{\tau}$ that of the additional stress tensor and \dot{y} is a measure of the shear rate that is defined by:

$$\dot{y} = \sqrt{\frac{1}{2} \sum_{i,j} \dot{y}_{ij} \dot{y}_{ji}} = \sqrt{\frac{1}{2} \Pi} \tag{10}$$

where, Π represents the second invariant of the tensor of strain rate. In the constitutive equation, we take into account (3.6). The argument in favor of which $\mu_\infty = 0$ and in order for us to write

$$\bar{\tau} = -\mu_0 [(1 + (\bar{\Gamma} \dot{y})^2)^{\frac{n-1}{2}}] \dot{y} \tag{11}$$

That is, if ($n=1$ or $\bar{\Gamma} = 0$) we reduced the form to the Newtonian fluid so, the elements that make up shear stress $\bar{\tau}$ within the confines of a predetermined structure can also be expressed as:

$$\begin{aligned}
\bar{\tau}_{\bar{X}\bar{Y}} &= \mu_0 [1 + (\frac{n-1}{2} (\bar{\Gamma} \dot{y})^2)] \cdot \frac{\partial \bar{U}}{\partial \bar{Y}} \\
\frac{\partial \bar{U}}{\partial \bar{Y}} &= \dot{y}
\end{aligned} \tag{12}$$

Substituting (5) into Eqs. (3)-(12), we obtain the following:

$$0 = -\frac{\partial p}{\partial x} + \frac{\partial}{\partial y} t_{xy} - (M^2 \cos^2(\beta) u + k^2) \frac{\partial \psi}{\partial y} + \Gamma \sin \alpha \tag{14}$$

$$\text{Repr} \left(\frac{\partial \theta}{\partial t} + u \frac{\partial \theta}{\partial x} \right) = \frac{\partial^2 \theta}{\partial y^2} + \text{Br} t_{xy} \frac{\partial u}{\partial y} - \text{Br} M^2 \cos^2(\beta) u^2 \tag{15}$$

Considering the in accordance with the following boundary conditions:

$$\left. \begin{aligned} u &= 1, \text{ at } (y = 1) \\ \frac{\partial u}{\partial y} &= \alpha_1 \text{Dru}, \text{ at } (y = -1) \end{aligned} \right\} \tag{16}$$

$$\left. \begin{aligned} \frac{\partial \theta}{\partial y} &= \text{Bh} \theta \text{ at } y = -1 \\ \frac{\partial \theta}{\partial y} &= \text{Bh}(1 - \theta) \text{ at } y = 1 \end{aligned} \right\} \tag{17}$$

$$\tau_{xy} = \frac{\partial u}{\partial y} + \left(\frac{n-1}{2} \right) (we)^2 \left(\frac{\partial u}{\partial y} \right)^3, \dot{y} = \frac{\partial u}{\partial y} \tag{18}$$

Now, if we take the Reynolds number as small and less than one, we have:

$$0 = -\frac{\partial p}{\partial x} + \frac{\partial}{\partial y} t_{xy} - (M^2 \cos^2(\beta) u + \Gamma \sin \alpha) \tag{19}$$

$$0 = \frac{\partial^2 \theta}{\partial y^2} + \text{Br} t_{xy} \frac{\partial u}{\partial y} - \text{Br} M^2 \cos^2(\beta) u^2 \tag{20}$$

In the Couette flow, we assume that the pressure gradient between parallel plates is zero. Thus, Eq. (19) can be taken the following formula:

$$0 = \frac{\partial}{\partial y} \left(\frac{\partial u}{\partial y} + \left(\frac{n-1}{2} \right) (we)^2 \left(\frac{\partial u}{\partial y} \right)^3 \right) - (M^2 \cos^2(\beta) u + \Gamma \sin \alpha) \tag{21}$$

$$0 = \frac{\partial^2 u}{\partial y^2} + 3(we)^2 \left(\frac{n-1}{2} \right) \left(\frac{\partial u}{\partial y} \right)^2 \cdot \frac{\partial^2 u}{\partial y^2} - (M^2 \cos^2(\beta) u + \Gamma \sin \alpha) \tag{22}$$

5. PROBLEM'S SOLUTION

5.1 Solution of moment equation

It's obvious that the produced formula for motion (Eq. (22)) is not linear, so it is difficult to find the solution exactly. Thus, we have to solve the equation approximately by using (RPTM), and we obtain a series of solutions for the axial velocity. We expand u for small Weissenberg numbers, the following is true:

$$u = u_0 + (we)^2 u_1 + O((we)^2) \tag{23}$$

Substituting Eq. (23) into Eq. (22) and boundary conditions (16), the following ranking of systems is obtained.

5.1.1 The zero-based ordering system $w e^{(0)}$

$$0 = \frac{\partial^2 u_0}{\partial y^2} - M^2 \cos^2(\beta) u_0 + \Gamma \sin \alpha \quad (24)$$

Together with the related boundary conditions:

$$\left. \begin{aligned} u_0 &= 1, \text{ at } (y = 1) \\ \frac{\partial u_0}{\partial y} &= \alpha_1 \text{Dru}_0, \text{ at } (y = -1) \end{aligned} \right\} \quad (25)$$

5.1.2 System of order two ($w e^{(2)}$)

$$0 = \frac{\partial^2 u_1}{\partial y^2} + 3 \left(\frac{n-1}{2} \right) \left(\frac{\partial u_0}{\partial y} \right)^2 \cdot \frac{\partial^2 u_0}{\partial y^2} - M^2 \cos^2(\beta) u_1 \quad (26)$$

$$\left. \begin{aligned} u_1 &= 1, \text{ at } (y = 1) \\ \frac{\partial u_1}{\partial y} &= \alpha_1 \text{Dru}_1, \text{ at } (y = -1) \end{aligned} \right\} \quad (27)$$

5.1.3 Solution of order zero

The solution of Eq. (24) subject to the corresponding boundary conditions (25) is taken the form:

$$u_0 = e^{N_1 y} a_1 + e^{-N_1 y} a_2 + \frac{\Gamma \text{Sin}[\alpha]}{N_1^2}; \quad (28)$$

5.1.4 Solution of order two

The solution of Eq. (26) subject to the corresponding boundary conditions (27) is taken the form:

$$\begin{aligned} u_1 &= \frac{3}{16} a_2^3 e^{-3N_1 y} N_1^2 + \frac{3}{8} a_1 a_2^2 e^{-N_1 y} N_1^2 + \frac{3}{8} a_1^2 a_2 e^{N_1 y} N_1^2 \\ &+ \frac{3}{16} a_1^3 e^{3N_1 y} N_1^2 - \frac{3}{16} a_2^3 e^{-3N_1 y} n N_1^2 - \frac{3}{8} a_1 a_2^2 e^{-N_1 y} n N_1^2 \\ &- \frac{3}{8} a_1^2 a_2 e^{N_1 y} n N_1^2 - \frac{3}{16} a_1^3 e^{3N_1 y} n N_1^2 + \frac{3}{4} a_1 a_2^2 e^{-N_1 y} N_1^3 y \\ &- \frac{3}{4} a_1^2 a_2 e^{N_1 y} N_1^3 y - \frac{3}{4} a_1 a_2^2 e^{-N_1 y} n N_1^3 y + \frac{3}{4} a_1^2 a_2 e^{N_1 y} n \\ &N_1^3 y + e^{N_1 y} b_1 + e^{-N_1 y} b_2; \end{aligned} \quad (29)$$

where, $b_j(j=1,2)$ an optional constant can be found by using boundary conditions (27), therefore, the solution of fluid's velocity can be obtained by:

$$\begin{aligned} u &= a_2 e^{-N_1 y} + a_1 e^{N_1 y} + w e^2 (b_2 e^{-N_1 y} + b_1 e^{N_1 y}) + \frac{3}{16} \\ &a_2^3 e^{-3N_1 y} N_1^2 + \frac{3}{8} a_1 a_2^2 e^{-N_1 y} N_1^2 + \frac{3}{8} a_1^2 a_2 e^{N_1 y} N_1^2 + \\ &\frac{3}{16} a_1^3 e^{3N_1 y} N_1^2 - \frac{3}{16} a_2^3 e^{-3N_1 y} n N_1^2 - \frac{3}{8} a_1 a_2^2 e^{-N_1 y} \\ &n N_1^2 - \frac{3}{8} a_1^2 a_2 e^{N_1 y} n N_1^2 - \frac{3}{16} a_1^3 e^{3N_1 y} n N_1^2 + \frac{3}{4} a_1 a_2^2 \\ &e^{-N_1 y} N_1^3 y - \frac{3}{4} a_1^2 a_2 e^{N_1 y} N_1^3 y - \frac{3}{4} a_1 a_2^2 e^{-N_1 y} n N_1^3 y \\ &+ \frac{3}{4} a_1^2 a_2 e^{N_1 y} n N_1^3 y) + n^2 \Gamma \text{Sin}[\alpha]; \end{aligned} \quad (30)$$

5.2 Thermodynamic equation and its solution

The solution of the energy equation (Eq. (20)) can be solved numerically using the method of "Explicit Euler" with size step by (0.1) by using the Mathematica program. The numerical results have mentioned in Tables 1-11 for different types of parameters.

Table 1. Variation of temperature θ with y for different values of M

y	M=0.1	M=0.15	M=0.2
0.1	1.62383	1.64689	1.67868
0.2	1.61771	1.64109	1.67333
0.3	1.60629	1.62973	1.66207
0.4	1.58999	1.61322	1.64531
0.5	1.56917	1.59193	1.62339
0.6	1.54411	1.56614	1.59661
0.7	1.51505	1.53609	1.5652
0.8	1.48212	1.50192	1.52933
0.9	1.44541	1.46374	1.48913
1	1.40492	1.42159	1.44467

Table 2. Variation of temperature θ with y for different values of Nr

y	Nr=0.1	Nr=0.2	Nr=0.25
0.1	1.16315	1.21599	1.25869
0.2	1.16622	1.2185	1.26073
0.3	1.1667	1.21804	1.25951
0.4	1.16491	1.21495	1.25535
0.5	1.16111	1.20948	1.24851
0.6	1.1555	1.20183	1.23921
0.7	1.14824	1.19217	1.22761
0.8	1.13945	1.18062	1.21383
0.9	1.12917	1.16723	1.19793
1	1.11743	1.15203	1.17993

Table 3. Variation of temperature θ with y for different values of β

y	$\beta=0$	$\beta=\frac{\pi}{6}$	$\beta=\frac{\pi}{4}$
0.1	1.78682	1.74312	1.69831
0.2	1.78314	1.73874	1.69325
0.3	1.77239	1.72775	1.68206
0.4	1.75493	1.71054	1.66515
0.5	1.73105	1.68742	1.64286
0.6	1.70104	1.65869	1.61547
0.7	1.66514	1.62458	1.58323
0.8	1.62356	1.58529	1.54632
0.9	1.5765	1.541	1.50488
1	1.52409	1.49182	1.45898

Table 4. Variation of temperature θ with y for different values of α

y	$\alpha=\frac{\pi}{9}$	$\alpha=\frac{\pi}{8}$	$\alpha=\frac{\pi}{7}$
0.1	1.66293	1.67803	1.7025
0.2	1.66486	1.6783	1.70072
0.3	1.65995	1.67182	1.69227
0.4	1.64848	1.65889	1.67749
0.5	1.63071	1.63981	1.65669
0.6	1.60689	1.61484	1.63016
0.7	1.57728	1.58424	1.59815
0.8	1.54211	1.54825	1.56089
0.9	1.50161	1.5071	1.5186
1	1.45601	1.461	1.47146

Table 5. Variation of temperature θ with y for different values of Da

y	$Da=3$	$Da=3.5$	$Da=4$
0.1	1.54351	1.57152	1.59406
0.2	1.54595	1.57309	1.59493
0.3	1.54265	1.56876	1.58979
0.4	1.53386	1.55882	1.57893
0.5	1.51982	1.54351	1.56261
0.6	1.50074	1.52306	1.54106
0.7	1.4768	1.49765	1.51449
0.8	1.44814	1.46747	1.48308
0.9	1.4149	1.43266	1.447
1	1.37718	1.39332	1.40636

Table 6. Variation of temperature θ with y for different values of α_1

y	$\alpha_1=1$	$\alpha_1=1.2$	$\alpha_1=1.4$
0.1	1.69851	1.74646	1.78446
0.2	1.69669	1.74308	1.77988
0.3	1.68838	1.73296	1.76836
0.4	1.67389	1.71644	1.75026
0.5	1.65349	1.69383	1.72591
0.6	1.62744	1.6654	1.69561
0.7	1.59593	1.63137	1.6596
0.8	1.55913	1.59195	1.61812
0.9	1.51717	1.5473	1.57133
1	1.47015	1.49755	1.51939

Table 7. Variation of temperature θ with y for different values of Br

y	$Br=1.5$	$Br=1.6$	$Br=1.7$
0.1	1.65501	1.71076	1.76651
0.2	1.65422	1.70836	1.7625
0.3	1.64714	1.69939	1.75163
0.4	1.63407	1.68417	1.73428
0.5	1.61529	1.66302	1.71075
0.6	1.59103	1.63618	1.68133
0.7	1.56153	1.60389	1.64625
0.8	1.52694	1.56634	1.60574
0.9	1.48743	1.5237	1.55997
1	1.44312	1.47609	1.50906

Table 8. Variation of temperature θ with y for different values of Bh

y	$Bh=1.4$	$Bh=1.5$	$Bh=1.6$
0.1	1.42664	1.37661	1.3342
0.2	1.43048	1.38192	1.34084
0.3	1.42828	1.3813	1.34166
0.4	1.42037	1.3751	1.33699
0.5	1.40705	1.36358	1.3271
0.6	1.38857	1.34701	1.31223
0.7	1.36514	1.3256	1.29261
0.8	1.33694	1.2995	1.26838
0.9	1.30411	1.26887	1.23969
1	1.26677	1.2338	1.20663

Table 9. Variation of temperature θ with y for different values of Γ

y	$\Gamma=0.8$	$\Gamma=0.9$	$\Gamma=1$
0.1	1.70844	1.73458	1.76651
0.2	1.70842	1.73255	1.7625
0.3	1.70146	1.72363	1.75163
0.4	1.68784	1.70816	1.73428

0.5	1.66786	1.68643	1.71075
0.6	1.64177	1.65874	1.68133
0.7	1.60983	1.62532	1.64625
0.8	1.57228	1.58642	1.60574
0.9	1.52934	1.54223	1.55997
1	1.48122	1.49294	1.50906

Table 10. Variation of temperature θ with y for different values of we

y	$we=0.1$	$we=0.18$	$we=0.2$
0.1	3.59513	3.54726	3.53388
0.2	3.55658	3.50598	3.49186
0.3	3.50647	3.45343	3.43865
0.4	3.44442	3.38938	3.37405
0.5	3.36952	3.31303	3.29731
0.6	3.28025	3.22304	3.20713
0.7	3.17455	3.11753	3.10169
0.8	3.04979	2.99415	2.9787
0.9	2.90279	2.85002	2.83538
1	2.72981	2.68184	2.66853

Table 11. Variation of temperature θ with y for different values of n

y	$n=10$	$n=12$	$n=14$
0.1	1.93216	1.96191	1.99114
0.2	1.92573	1.95521	1.98417
0.3	1.91103	1.93998	1.96845
0.4	1.88851	1.91668	1.94441
0.5	1.85859	1.88576	1.91252
0.6	1.8217	1.84763	1.87321
0.7	1.77821	1.80271	1.82689
0.8	1.7285	1.75138	1.77398
0.9	1.67291	1.694	1.71485
1	1.61174	1.63091	1.64986

6. DISCUSSION OF THE RESULTS

This section will be created to discuss the impact that embedded parameters, like Hartmann and Darcy numbers, the angle at which a magnetic field tilts β , the sloping angle of the channel α , slip parameter α_1 , power law index n , weissenberg number (we), Brinkman number (Br), heat transfer Biot number (Bh) and the parameter $\Gamma = \frac{Re}{Fr}$ on the velocity and heat characteristics.

6.1 Velocity distribution

Figures 2-9 are prepared to show the effect of parameters ($M, \beta, Dr, n, \Gamma, \alpha, \alpha_1, we$) on the velocity characteristics. From Figure 2, we can deduce that the flow velocity decreases as the Hartmann number M rises. This is because the Lorentz force, a factor that works against the current and reduces the fluid's velocity, determines the Hartmann number [6]. The velocity of the Carreau fluid decreases as the power-law index and the weissenberg number (we) increase, as seen in Figures 3 and 4. That is, Newtonian fluid (when $n=1$ or $we=0$) is more than Carreau fluid. The effect of the inclination angle of the magnetic field β on the flow is shown in Figure 5. It can be seen that this parameter has an increasing effect on the velocity. This is mostly due to the fact that an increase in the magnetic field inclination angle causes a reduction in the lagging behind the impact of the Lorentz force. As a consequence, the magnetic field that is being utilized in relation to the flow will

also diminish, and its influence will be minimal. Figure 6 displayed the effect of darcy number (Dr), in which an increase in this parameter led to a reduction in the velocity of the fluid. This observation is supported by the laws of physics due to the fact that a more permeable porous media offers less resistance to the flow of fluid; as a result, there is a discernible quickening in the fluid's rate of motion. The effect of the slip parameter α_1 produces behavior that is comparable to that observed on the velocity, and its impact is shown in Figure 7 the same case of Darcy and slip parameters effects is found in [17]. The affirmative impress is observed by the impact of parameters Γ and the slant of the canal α on the velocity and is drawn in Figures 8 and 9, respectively.

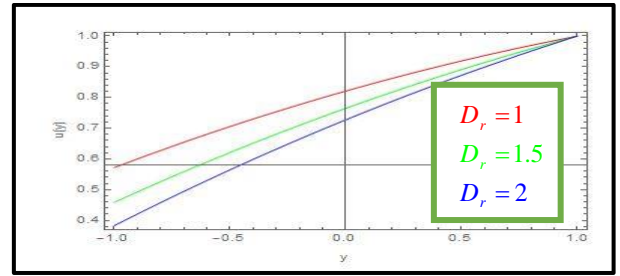


Figure 6. Effect of Dr on velocity $we=0.01, n=2, M=0.2, \beta=\pi/4, \alpha_1=0.5, \Gamma=0.1, \alpha=\pi/3$

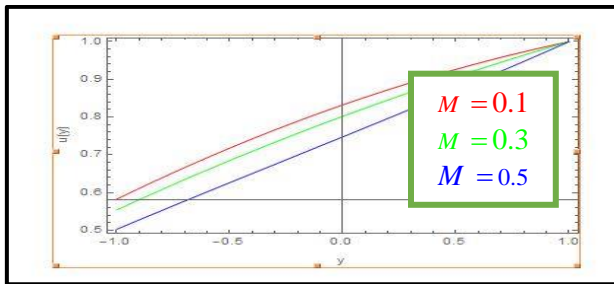


Figure 2. Effect of M on velocity $we=0.01, n=2, \Gamma=0.1, \alpha_1=0.5, \beta=\pi/4, Dr=1, \alpha=\pi/3$

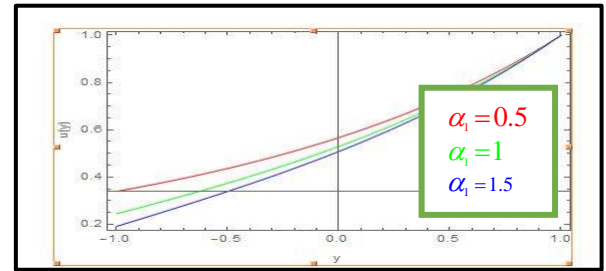


Figure 7. Effect of α_1 on velocity $we=0.01, n=2, M=1, \Gamma=0.1, \beta=\pi/4, Dr=1, \alpha=\pi/3$

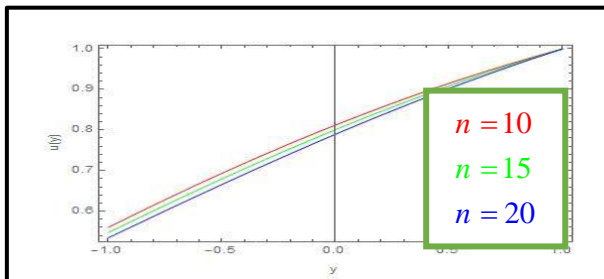


Figure 3. Effect of n on velocity $we=0.01, M=0.1, \Gamma=0.1, \alpha_1=0.5, \beta=\pi/4, Dr=1, \alpha=\pi/3$

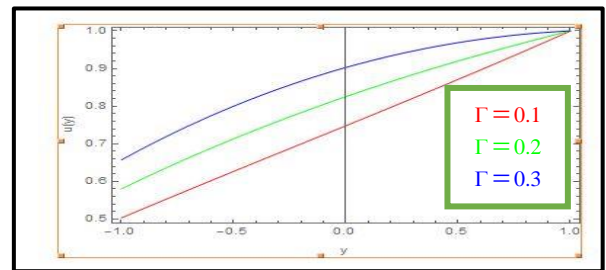


Figure 8. Effect of Γ on velocity $we=0.01, n=2, M=0.5, \alpha_1=0.5, \beta=\pi/4, Dr=1, \alpha=\pi/3$

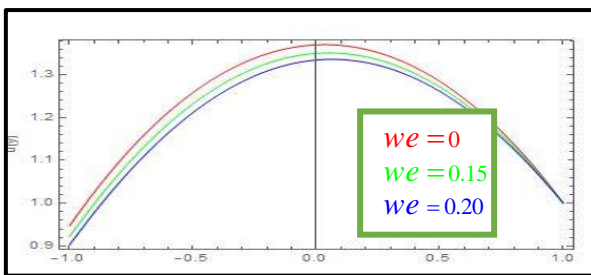


Figure 4. Effect of we on velocity $M=0.7, Dr=1, \alpha = \frac{\pi}{4}, \beta = \frac{\pi}{4}, \alpha_1=0.5, \Gamma=0.1, n=2$

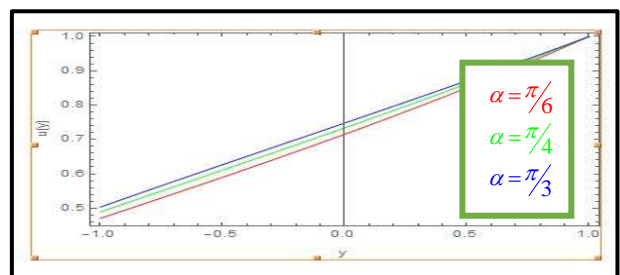


Figure 9. Effect of α on velocity $we=0.01, n=2, M=0.5, Dr=1, \alpha_1=0.5, \Gamma=0.1, \beta=\frac{\pi}{4}$

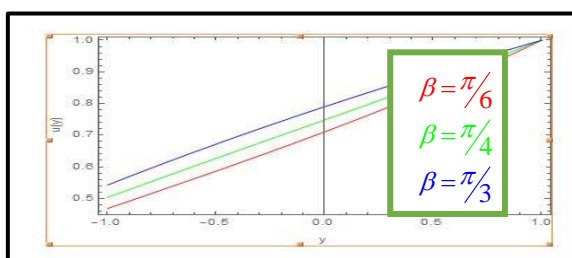


Figure 5. Effect of β on velocity $we=0.01, n=2, M=0.5, \alpha_1=0.5, \Gamma=0.1, Dr=1, \alpha=\pi/3$

6.2 Temperature distribution

To study the impact of the variables involved in the problem, like ($M, \beta, Dr, \eta, \Gamma, \alpha, \alpha_1, we, Bh, Br, Nr$), on heat characteristics, Figures 10-20 have been plotted. It stands to reason that in a flow of a viscous fluid, the energy contained in the motion of the fluid will be converted by the viscosity of the fluid into internal energy, resulting in an increase in temperature. The relevance of magnetic field inclination β on temperature is shown in Figure 10. It can be seen from the image that the temperature is a function that decreases as this parameter does. The reason for this is that a fluid that conducts electricity is subject in opposition to a force called the Lorentz

force, which is generated when a transverse magnetic field is applied to it. Because of this force, the fluid will suffer resistance, which will increase the friction that occurs between its layers, and as a result, the temperature of the fluid will decrease. The reverse behavior has been observed for the impact of the Hartmann number on the M fluid's temperature, and its effect is sketched in Figure 11. The same proceeding is displayed in Figure 12 for the impress of parameter Γ on the fluid's temperature, and the function of temperature is an increasing function of M and Γ respectively. Figures 13 and 14 are plotted for the action of slant or slanting of channel α and Darcy number (Dr.) on temperature distribution. It is made out that an increase in values of these parameters results in a raise in the magnitude of the fluid's temperature, which means that the higher rate of porous media shows heat more clearly than Clear medium. The impact of the power index n and slip parameter α_1 is seen in Figures 15 and 16, respectively. It is examined that these parameters have a growing effect on the temperature of the fluid. That is, the temperature of the fluid exhibiting Newtonian behavior ($n=1$) is less than non-Newtonian Carreau fluid ($n \neq 1$).

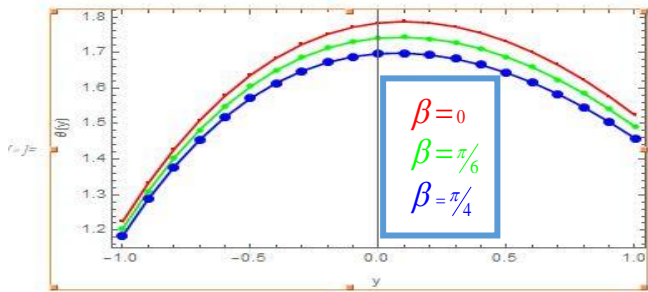


Figure 10. Effect of β on temperature $n=0.5$, $we=0.01$, $M=0.3$, $\alpha=\pi/6$, $Da=3$, $\alpha_1=1.3$, $Nr=0.5$, $Br=1.7$, $Bh=1$, $\Gamma=1$

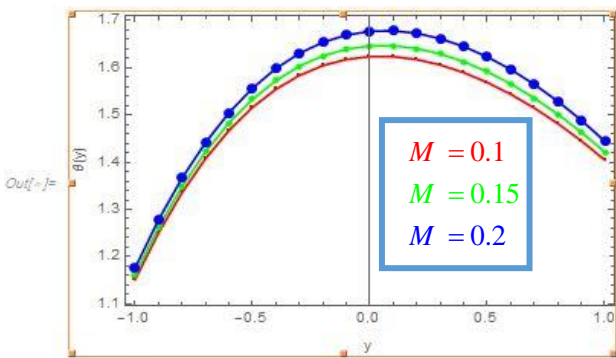


Figure 11. Effect of M on temperature $n=0.5$, $we=0.01$, $\beta=\pi/9$, $\alpha=\pi/6$, $Da=3$, $\alpha_1=1.3$, $Nr=0.5$, $Br=1.7$, $Bh=1$, $\Gamma=1$

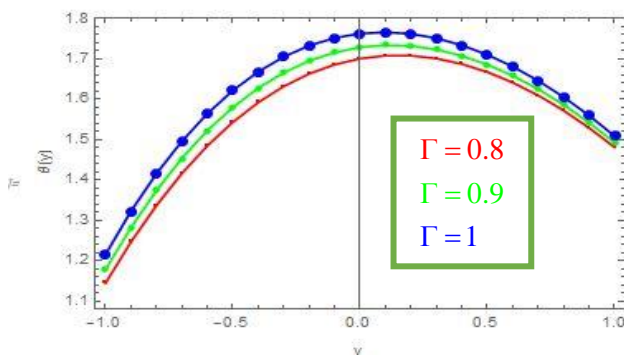


Figure 12. Effect of Γ on temperature $n=0.5$, $we=0.01$, $\beta=\pi/9$, $\alpha=\pi/6$, $Da=3$, $\alpha_1=1.3$, $Nr=0.5$, $Br=1.7$, $Bh=1$, $M=0.3$

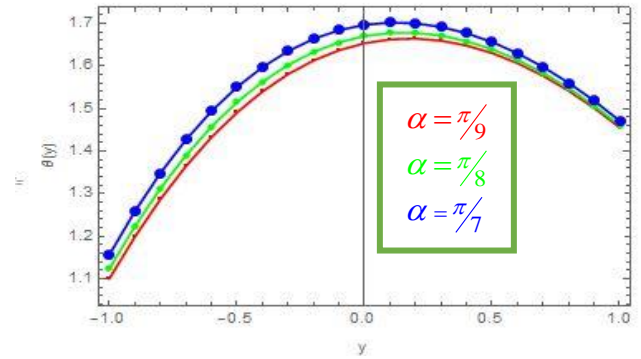


Figure 13. Effect of α on temperature $n=0.5$, $we=0.01$, $\beta=\pi/9$, $\Gamma=1$, $Da=3$, $\alpha_1=1.3$, $Nr=0.5$, $Br=1.7$, $Bh=1$, $M=0.3$

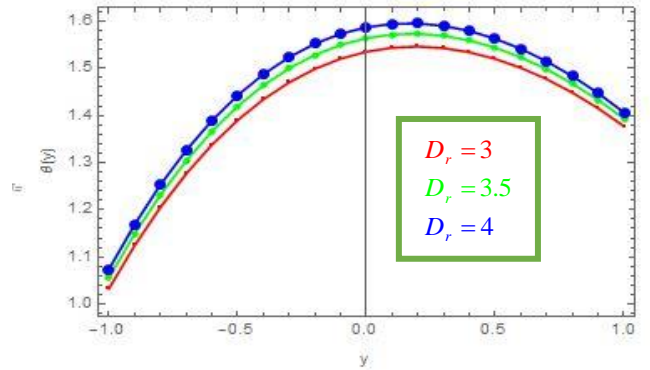


Figure 14. Effect of Dr on temperature $n=0.5$, $we=0.01$, $\beta=\pi/9$, $\alpha=\pi/6$, $\Gamma=1$, $\alpha_1=1.3$, $Nr=0.5$, $Br=1.7$, $Bh=1$, $M=0.3$

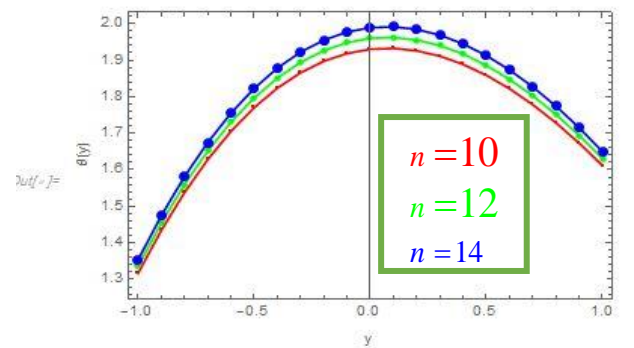


Figure 15. Effect of n on temperature $Da=3$, $we=0.01$, $\beta=\pi/9$, $\alpha=\pi/6$, $\Gamma=1$, $\alpha_1=1.3$, $Nr=0.5$, $Br=1.7$, $Bh=1$, $M=0.3$

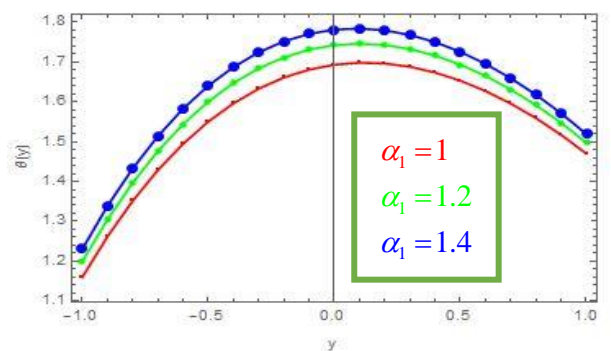


Figure 16. Effect of α_1 on temperature $n=0.5$, $we=0.01$, $\beta=\pi/9$, $\alpha=\pi/6$, $\Gamma=1$, $Da=3$, $Nr=0.5$, $Br=1.7$, $Bh=1$, $M=0.3$

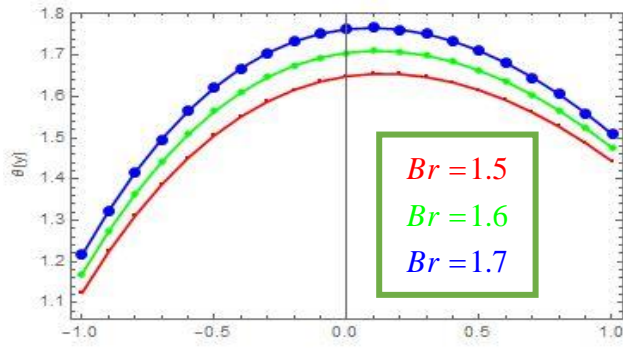


Figure 17. Effect of Br on temperature $n=0.5$, $we=0.01$, $\beta=\pi/9$, $\alpha=\pi/6$, $\Gamma=1$, $Da=3$, $Nr=0.5$, $\alpha_1=1.3$, $Bh=1$, $M=0.3$

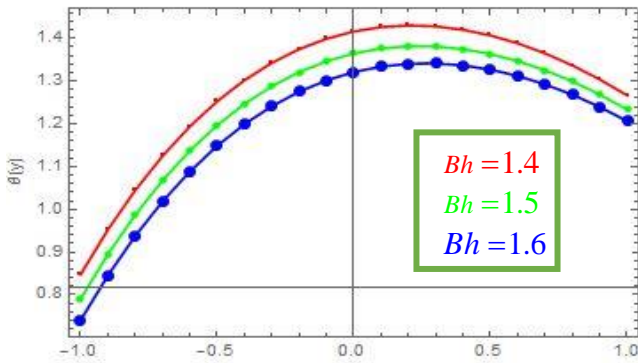


Figure 18. Effect of Bh on temperature $n=0.5$, $we=0.01$, $Bh=\pi/9$, $\alpha=\pi/6$, $\Gamma=1$, $Da=3$, $Nr=0.5$, $\alpha_1=1.3$, $Br=1.7$, $M=0.3$

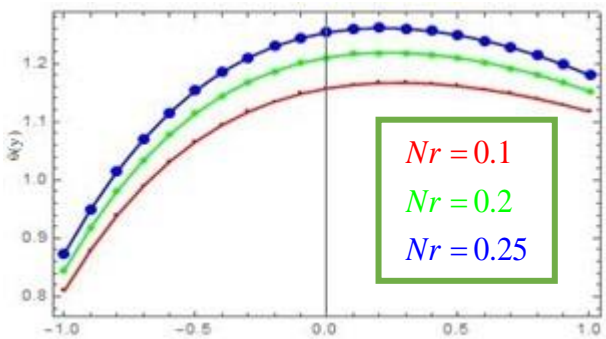


Figure 19. Effect of Nr on temperature $n=0.5$, $we=0.01$, $\beta=\pi/9$, $\alpha=\pi/6$, $\Gamma=1$, $Da=3$, $Bh=1$, $\alpha_1=1.3$, $Br=1.7$, $M=0.3$

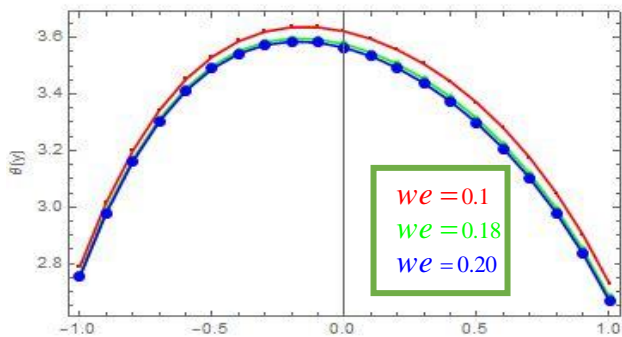


Figure 20. Effect of we on temperature $n=0.5$, $Nr=0.5$, $\beta=\pi/9$, $\alpha=\pi/6$, $\Gamma=1$, $Da=3$, $Bh=1$, $\alpha_1=1.3$, $Br=1.7$, $M=0.3$

Also, the temperature of the Carreau fluid in this study by using the effect of the slip parameter is more than the non-slip

parameter on boundary conditions of the flow [6]. A similar action is noticed in Figure 17 for the augment leverage of Brinkman number (Br) performed to enhance. The temperature of the liquid is measured. As the Brinkman number grows, the fluid's temperature rises because of the increased resistance to shear in the flow. It makes everything even hotter, generated by the impacts of viscous dissipation [27]. The converse case is shown in Figure 18 for the impress of Biot number (Bh) on temperature characteristics, which gives a decreased effect on fluid's temperature. It is due to the reduction of thermal conductivity [27]. The effect of the radiation parameter (Nr) is plotted in Figure 19. It is examined that the temperature of the fluid is an increasing function of (Nr). It is known that (Nr) defines the proportional importance of the contribution of conducting heat transfer to thermal radiation transfer, which gives the reason for the rising rate of fluid's temperature with an increase in values of this parameter [6]. The impact of the weissenberg number (we) on the temperature distribution is studied through Figure 20, which shows unfavorable action on the temperature of the fluid, that an increase in this parameter led to a decrease in the magnitude of fluid temperature, but this effect is starting to decay in the ends of fixed plate of the channel (lower-wall), that means that the medium of the flow in presence of Carreau fluid is less than for the flow of Newtonian fluid ($we=0$) [6].

7. CONCLUSION

The present study focuses on the investigation of a fundamental flow known as Couette flow. This flow involves an incompressible MHD Carreau fluid that is confined between parallel plates within an inclined channel. Notably, the bottom section of the channel is lined with a porous material. In this study, the slip boundary conditions on the flow are carefully considered. The present study also includes an examination of heat transfer, wherein convective boundary conditions are employed. The primary focus of this investigation revolves around identifying the key issues associated with the topic at hand.

1. Velocity is an increasing function of the variables (β , Γ , α) while the situation is covered by the variables (M , n , α_1 , Dr , we).
2. The temperature profile is an increasing function of the variables (M , Γ , α , Dr , Br , α_1 , n , Nr) and the trend is reversed of the variables (β , we , Bh).
3. The findings of the Newtonian model of fluids are captured from our analysis by putting ($n=1$ or $we=0$).

8. POTENTIAL AREA FOR FUTURE WORK

1. We can use variable of dynamic viscosity of conducting Carreau fluid on the Couette flow.
2. We can use generalize Couette flow of conducting Carreau fluid under the same condition.
3. We can make comparison between two different flows (Couette & Poiseuille) of conducting Carreau fluid. Under the same conditions.

REFERENCES

- [1] Bhatti, M.M., Zeeshan, A. (2016). Analytic study of heat

- transfer with variable viscosity on solid particle motion in dusty Jeffery fluid. *Modern Physics Letters B*, 30(16): 1650196. <https://doi.org/10.1142/S0217984916501967>
- [2] Srinivas, S., Muthuraj, R. (2010). Peristaltic transport of a Jeffery fluid under the effect of slip in an inclined asymmetric channel. *International Journal of Applied Mechanics*, 2(2): 437-455. <https://doi.org/10.1142/S1758825110000573>
- [3] Akbar, N.S., Nadeem, S., Ali, M. (2011). Jeffrey fluid model for blood flow through a tapered artery with a stenosis. *Journal of Mechanics in Medicine and Biology*, 11(3): 529-545. <https://doi.org/10.1142/S0219519411003879>
- [4] Abdulhadi, A.M., Ahmed, T.S. (2017). Effect of magnetic field on peristaltic flow of Williamson fluid through a porous medium in an inclined tapered asymmetric channel. *Mathematical Theory and Modeling*, 7(5): 49-65.
- [5] Hayat, T., Yasmin, H., Alsaedi, A. (2014). Peristaltic motion of Carreau fluid in a channel with convective boundary conditions. *Applied Bionics and Biomechanics*, 11(3): 157-168. <https://doi.org/10.3233/ABB-140094>
- [6] Ramesh, K. (2018). Effects of viscous dissipation and Joule heating on the Couette and Poiseuille flows of a Jeffrey fluid with slip boundary conditions. *Propulsion and Power Research*, 7(4): 329-341. <https://doi.org/10.1016/j.jprr.2018.11.008>
- [7] Akbar, N.S., Tripathi, D., Bég, O.A., Khan, Z.H. (2016). MHD dissipative flow and heat transfer of Casson fluids due to metachronal wave propulsion of beating cilia with thermal and velocity slip effects under an oblique magnetic field. *Acta Astronautica*, 128: 1-12. <https://doi.org/10.1016/j.actaastro.2016.06.044>
- [8] Hayat, T., Saleem, N., Ali, N. (2010). Effect of induced magnetic field on peristaltic transport of a Carreau fluid. *Communications in Nonlinear Science and Numerical Simulation*, 15(9): 2407-2423. <https://doi.org/10.1016/j.cnsns.2009.09.032>
- [9] Prakash, J., Balaji, N., Siva, E.P., Kothandapani, M., Govindarajan, A. (2018). Effects of magnetic field on peristalsis transport of a Carreau fluid in a tapered asymmetric channel. *Journal of Physics: Conference Series*, 1000(1): 012166. <http://doi.org/10.1088/1742-6596/1000/1/012166>
- [10] Ahmed, T.S. (2018). Effect of inclined magnetic field on peristaltic flow of Carreau fluid through porous medium in an inclined tapered asymmetric channel. *Al-Mustansiriyah Journal of Science*, 29(3): 94-105. <http://doi.org/10.23851/mjs.v29i3.641>
- [11] Abdulhadi, A.M., Ahmed, T.S. (2018). Effect of radial magnetic field on peristaltic transport of Jeffrey fluid in curved channel with heat/mass transfer. *Journal of Physics: Conference Series*, 1003(1): 012053. <https://doi.org/10.1088/1742-6596/1003/1/012053>
- [12] Adnan, F.A., Hadi, A.M.A. (2019). Effect of an inclined magnetic field on peristaltic flow of Bingham plastic fluid in an inclined symmetric channel with slip conditions. *Iraqi Journal of Science*, 60(7): 1551-1574. <https://doi.org/10.24996/ij.s.2019.60.7.16>
- [13] Abdulhadi, A.M., Al-hadad, A.H. (2015). Slip effect on the peristaltic transport of MHD fluid through a porous medium with variable viscosity. *Iraqi Journal of Science*, 56(3B): 2346-2363.
- [14] Abdulhadi, A.M., Al-Hadad, A.H. (2016). Effects of rotation and MHD on the nonlinear peristaltic flow of a Jeffery fluid in an asymmetric channel through a porous medium. *Iraqi Journal of Science*, 57(1A): 223-240.
- [15] Salih, A.W., Habeeb, S.B. (2022). Peristaltic flow with nanofluid under effects of heat source, and inclined magnetic field in the tapered asymmetric channel through a porous medium. *Iraqi Journal of Science*, 63(10): 4445-4459. <https://doi.org/10.24996/ij.s.2022.63.10.30>
- [16] Mokarizadeh, H., Asgharian, M., Raisi, A. (2013). Heat transfer in Couette-Poiseuille flow between parallel plates of the Giesekus viscoelastic fluid. *Journal of Non-Newtonian Fluid Mechanics*, 196: 95-101. <https://doi.org/10.1016/j.jnnfm.2013.01.007>
- [17] Reddappa, B., Sreenadh, S., Naidu, K.K. (2015). Convective Couette flow of a Jeffrey fluid in an inclined channel when the walls are provided with porous lining. *Advances in Applied Science Research*, 6(12): 69-75.
- [18] Channabasappa, M.N., Umapathy, K.G., Nayak, I.V. (1976). The effect of the thickness of the porous material on the parallel plate channel flow when the walls are provided with non-erodible porous lining. *Applied Scientific Research*, 32: 607-617. <https://doi.org/10.1007/BF00384123>
- [19] Naidu, K.K.S., Sudhakara, E., Sreenadh, S., Arunachalam, P.V. (2014). The effect of the thickness of the porous material on the parallel plate channel flow of Jeffrey fluid when the walls are provided with non-erodible porous lining. *International Journal of Scientific and Innovative Mathematical Research*, 2(7): 627-636. <https://citeseerx.ist.psu.edu/document?repid=rep1&type=pdf&doi=4204f7e0ffb722322285a0aa5a0652e71cc4fd41>
- [20] Abedulhadi, T.S.A.A.M. (2017). Effect of magnetic field on peristaltic flow of jeffrey fluid through porous medium in a tapered asymmetric channel. *Global Journal of Mathematics*, 9(2). <https://www.gpcpublishing.com/wp>.
- [21] Nassief, A.M., Abdulhadi, A.M. (2023). Magnetic force for peristaltic transport of non-newtonian fluid through porous medium in asymmetric channel. *Iraqi Journal of Science*, 64(7): 3567-3586 2023. <https://doi.org/10.24996/ij.s.2023.64.7.35>
- [22] Khudair, W.S., Al-Khafajy, D. (2018). Influence of heat transfer on Magneto hydrodynamics oscillatory flow for Williamson fluid through a porous medium. *Iraqi Journal of Science*, 59(1B): 389-397. <https://doi.org/10.24996/ij.s.2018.59.1b.18>
- [23] Zhilenko, D., Krivonosova, O., Gritsevich, M., Read, P. (2018). Wave number selection in the presence of noise: Experimental results. *Chaos: An Interdisciplinary Journal of Nonlinear Science*, 28(5): 053110. <https://doi.org/10.1063/1.5011349>
- [24] Hayat, T., Khan, M., Ayub, M. (2004). Couette and Poiseuille flows of an Oldroyd 6-constant fluid with magnetic field. *Journal of mathematical analysis and applications*, 298(1): 225-244. <https://doi.org/10.1016/j.jmaa.2004.05.011>
- [25] Yabo, I.B., Jha, B.K., Lin, J.E. (2018). On a Couette flow of conducting fluid. *International Journal of Theoretical and Applied Mathematics*, 4(1): 8-21. <https://doi.org/10.11648/j.ijtam.20180401.12>
- [26] Ellahi, R., Shivanian, E., Abbasbandy, S., Hayat, T. (2016). Numerical study of magnetohydrodynamics

- generalized Couette flow of Eyring-Powell fluid with heat transfer and slip condition. *International Journal of Numerical Methods for Heat & Fluid Flow*, 26(5): 1433-1445. <https://doi.org/10.1108/HFF-04-2015-0131>
- [27] Nadeem, M., Siddique, I., Ali, R., Alshammari, N., Jamil, R.N., Hamadneh, N., Khan, I., Andualet, M. (2022). Study of third-grade fluid under the fuzzy environment with Couette and Poiseuille flows. *Mathematical Problems in Engineering*, 2022: 1-19. <https://doi.org/10.1155/2022/2458253>
- [28] Rickert, W., Vilchevskaya, E., Müller, W. (2019). A note on Couette flow of micropolar fluids according to Eringen's theory. *Mathematics and Mechanics of Complex Systems*, 7(1): 25-50. <https://doi.org/10.2140/memocs.2019.7.25>
- [29] Niranjana, N., Vidhya, M., Govindarajan, A. (2018). Couette flow of an incompressible fluid in a porous channel with mass transfer. *Journal of Physics: Conference Series*, 1000(1): 012007. <https://doi.org/10.1088/1742-6596/1000/1/012007>

NOMENCLATURE

we	Weissenberg number (parameter of Carreau fluid)
Nr	Radiation parameter
u	Velocity of the fluid
Dr	Darcy number

Bh	Heat transfer biot number
Re	Reynolds number
Ec	Eckert number
M	Hartmann number (parameter of a magnetic field)
Fr	Froud number
Pr	Taylor number
T_0	Plate temperature below
t	Time of the flow
$2h$	Distance between the plates of the channel
K_1	Thermal conductivity
T_1	Temperature of the plate located above.
g	Acceleration due to gravity
K_0	Permeability of the porous medium

Greek symbols

μ_0	Dynamic viscosity of the fluid
n	Power lower index
$\frac{\partial p}{\partial x}$	Pressure gradient
λ	Mean radiation absorption coefficient radiation parameter
ρ	Density of the fluid
α	The inclination angle of the channel to the horizontal
β	The inclination angle of the magnetic field
c_p	Specific heat capacity
α_1	Slip parameter